

Article

Cooperative Effects of Matrix Stiffness and Fluid Shear Stress on Endothelial Cell Behavior

Julie C. Kohn,¹ Dennis W. Zhou,¹ François Bordeleau,¹ Allen L. Zhou,¹ Brooke N. Mason,¹ Michael J. Mitchell,¹ Michael R. King,¹ and Cynthia A. Reinhart-King^{1,*}

¹Department of Biomedical Engineering, Cornell University, Ithaca, New York

ABSTRACT Arterial hemodynamic shear stress and blood vessel stiffening both significantly influence the arterial endothelial cell (EC) phenotype and atherosclerosis progression, and both have been shown to signal through cell-matrix adhesions. However, the cooperative effects of fluid shear stress and matrix stiffness on ECs remain unknown. To investigate these cooperative effects, we cultured bovine aortic ECs on hydrogels matching the elasticity of the intima of compliant, young, or stiff, aging arteries. The cells were then exposed to laminar fluid shear stress of 12 dyn/cm². Cells grown on more compliant matrices displayed increased elongation and tighter EC-cell junctions. Notably, cells cultured on more compliant substrates also showed decreased RhoA activation under laminar shear stress. Additionally, endothelial nitric oxide synthase and extracellular signal-regulated kinase phosphorylation in response to fluid shear stress occurred more rapidly in ECs cultured on more compliant substrates, and nitric oxide production was enhanced. Together, our results demonstrate that a signaling cross talk between stiffness and fluid shear stress exists within the vascular microenvironment, and, importantly, matrices mimicking young and healthy blood vessels can promote and augment the atheroprotective signals induced by fluid shear stress. These data suggest that targeting intimal stiffening and/or the EC response to intima stiffening clinically may improve vascular health.

INTRODUCTION

Mechanotransduction within the cardiovascular system is well studied but still not fully understood. It is well established that hemodynamic shear stress regulates atherosclerosis progression and the arterial endothelial cell (EC) phenotype (1,2). However, the shear stress studies conducted to date have largely been performed on ECs cultured on plastic or glass (3–5), which have significantly different compositions and mechanical properties compared with human vascular tissue (6). Evidence is now emerging that changes in vessel stiffness that occur with age, metabolic disorders, and atherosclerosis can promote an atherosclerotic phenotype in the cells within the vessel wall (6–9). Increased matrix stiffness from 2.5 to 10 kPa (mimicking age-related stiffening of the EC matrix) induces increased endothelium permeability and leukocyte transmigration, both of which are hallmarks of atherosclerosis progression (6). Although both fluid shear stress and matrix stiffness are implicated in atherosclerosis progression and signal through many of the same intracellular pathways (10,11), it is not yet known whether these mechanical cues can act synergistically to affect EC health.

Laminar arterial-level shear stress (10–30 dyn/cm²) is associated with an atheroprotective EC phenotype and causes ECs to align and elongate in the flow direction (1), which is

hypothesized to minimize EC resistance to fluid shear stress (12). In contrast, ECs exposed to low and oscillatory shear stress (<4 dyn/cm²), which is prevalent at atherosclerosis-prone arterial bifurcations, remain in a cobblestone-like formation (5). Fluid shear stress also affects multiple intracellular signaling pathways that can be atheroprotective. Notably, many of these pathways signal through focal adhesion kinase (FAK) (10), which has also been shown to be activated in response to increased matrix stiffness (13). Among the signaling molecules mediated by FAK, extracellular signal-regulated kinase (Erk1/2) (10), and endothelial nitric oxide synthase (eNOS) (14) play key roles in vascular homeostasis. Erk1/2 is known to regulate EC proliferation, and eNOS is responsible for producing the vasodilator nitric oxide (NO) (3,4,15), which has multiple atheroprotective effects. Laminar fluid shear stress is also known to activate both Erk1/2 and eNOS in ECs cultured on plastic or glass (3,16–18). Additionally, both ERK and eNOS have been shown to respond to mechanical stretch (19,20), suggesting that they are sensitive to mechanical cues from the extracellular matrix. ERK can mediate EC health by downregulating Rho-associated protein kinase (ROCK) (21), whereas eNOS phosphorylation has been shown to respond to ROCK activity (22), suggesting that matrix stiffness, which is known to affect the Rho-ROCK pathway, may influence shear-induced ERK and eNOS activity.

Here, we investigate the cooperative effects of matrix stiffness and fluid shear stress on EC health, with a specific focus on barrier integrity and NO production. Our data

Submitted May 7, 2014, and accepted for publication December 15, 2014.

*Correspondence: cak57@cornell.edu

Julie C. Kohn and Dennis W. Zhou contributed equally to this work.

Editor: Alan Grodzinsky.

© 2015 by the Biophysical Society

0006-3495/15/02/0471/8 \$2.00



indicate that compliant substrates mimicking the stiffness of young, healthy arteries enhance fluid shear-mediated EC alignment, barrier integrity, and eNOS and ERK signaling.

MATERIALS AND METHODS

Hydrogel preparation and cell culture

Polyacrylamide (PA) gels were prepared as described previously (6,23) and functionalized with 0.1 mg/mL rat tail collagen type I (BD Biosciences). Bovine aortic ECs (BAECs) between passages 6 and 12 were seeded on the PA gels of 2.5 or 10 kPa, or onto collagen-coated glass. The hydrogel substrates were chosen to mimic the mechanical properties of the subendothelial matrix in young and aged blood vessels (6,24). Samples were maintained with M199 media (Invitrogen) supplemented with 10% FetalClone III (HyClone) and 1% each of minimum essential media (MEM) amino acids (Invitrogen), MEM vitamins (Mediatech), and penicillin-streptomycin (Invitrogen). Samples were used at a minimum of 1 day postconfluence.

Administration of fluid shear stress

Three Brookfield DV-II+ Pro viscometers with the manufacturer's supplied CPE-40 cone (0.8°, 48 mm diameter) were validated as laminar shear stress models (Figs. S1 and S2 in the Supporting Material) as shown by previous studies (25,26). PA gels with confluent BAECs were fixed to the viscometer plate using a hydrophobic pen, vacuum grease, and silicone oil (Fig. S1). L-15 media (Invitrogen) with 1% penicillin-streptomycin and 10% FetalClone III was used for the shear stress experiments, with the addition of dextran (#95771; Sigma-Aldrich) at 29 mg/mL to increase media viscosity to 4 cP. Fluid shear stress of 12 ± 2 dyn/cm² was administered, using the equation below, for different time periods and media was replaced as necessary to compensate for evaporation during 24 h experiments.

$$\text{Shear Stress} = \tau = (\mu\omega)/\alpha = \mu * \text{ShearRate},$$

where α is the cone angle, μ is the viscosity, and ω is the angular velocity (25,26).

The viscometer temperature was maintained at $37^\circ\text{C} \pm 2^\circ\text{C}$ using a circulating water bath and hot plate. Static control groups with the same L-15 media were maintained at 37°C in an incubator with ambient CO₂ levels.

Cell morphology

Brightfield images were taken using a Zeiss Axiovert 40 C with a Zeiss AxioCam b/w 412-311 camera (Oberkochen, Germany) before shear stress exposure as well as after treatment. Samples underwent either static culture or shear of 12 dyn/cm² in L-15 media for 24 h. After treatment, cells were fixed in 3.7% formaldehyde (Alfa Aesar, Ward Hill, MA), washed in 1% Triton X-100 (Mallinckrodt Baker, Phillipsburg, NJ), and blocked with 4% bovine serum albumin (Sigma-Aldrich). Actin was stained with Alexa Fluor 568 phalloidin (Invitrogen), and nuclei were stained with 4',6-diamidino-2-phenylindole (DAPI; Sigma-Aldrich). Fluorescence images were captured on a Zeiss Axio Observer.Z1m microscope with a Hamamatsu ORCA-ER camera (Bridgewater, NJ). ImageJ was used to determine the cell perimeter and major/minor axis ratio (elongation). The images were also analyzed for other morphology parameters, such as cell alignment with the fluid flow direction (Fig. S3), using OrientationJ as described previously (27).

Junction width measurements

Samples underwent either static culture or shear of 12 dyn/cm² in L-15 media for 24 h. The samples were immunostained with goat polyclonal

VE-cadherin primary antibody (C-19; Santa Cruz Biotechnology, Santa Cruz, CA) and Alexa Fluor 568 donkey anti-goat secondary antibody (Invitrogen). Images were captured on a Zeiss Axio Observer.Z1m microscope with a Hamamatsu ORCA-ER camera. Junction width measurements were analyzed with ImageJ and a custom-written MATLAB (The MathWorks, Natick, MA) code as described previously (6). Briefly, using ImageJ, a line was drawn perpendicular to a randomly selected junction and the fluorescent intensity profiles were recorded. A one- or two-Gaussian curve was fit to the intensity profiles in MATLAB and junction widths were defined as the width of the Gaussian fit 20% above the background pixel intensity (28).

Erk1/2 and eNOS phosphorylation

Samples underwent shear of 12 dyn/cm² in L-15 media for 0, 2, 5, and 20 min. The BAECs were washed once with ice-cold phosphate-buffered saline (PBS), lysed with ice-cold modified radioimmunoprecipitation assay (RIPA) buffer (150 mM sodium chloride, 50 mM Tris-hydrochloride, 0.5% sodium deoxycholate, 0.1% sodium dodecyl sulfate, 1% Nonidet P40, 25 mM sodium fluoride, 1 mM sodium orthovanadate, 1:100 dilution of protease inhibitor cocktail; Sigma-Aldrich). Cell lysate was cleared by centrifugation at $14,000 \times g$ and the supernatant was separated by SDS-PAGE with 10 μg protein loading per lane. After the protein was transferred onto PVDF (Millipore, Billerica, MA), blots were probed using antibodies against phosphorylated endothelial NOS at Ser-1179 (p-eNOS, #9571; Cell Signaling Technology, Beverly, MA), total eNOS (#9572; Cell Signaling Technology), phosphorylated Erk1/2 at Thr-202/Tyr-204 (pErk, #9106; Cell Signaling Technology), and total Erk1/2 (#9102; Cell Signaling Technology) at the manufacturer's specified dilutions. Anti-rabbit or anti-mouse horseradish-peroxidase-conjugated secondary antibodies were obtained from Cell Signaling Technology. After incubation in SuperSignal West Pico chemiluminescent substrate (Thermo Scientific, Rockford, IL), blots were exposed and imaged using a FujiFilm ImageQuant LAS-4000. Protein densitometry was performed using ImageJ software.

Rho activation

For Rho activation, the same procedure described for Erk1/2 and eNOS phosphorylation was used. Cell lysates were collected after 0, 10, or 60 min of 12 dyn/cm² shear. Intracellular BAEC RhoA activity was quantified using a RhoA G-LISA kit (Cytoskeleton, Denver, CO) according to the manufacturer's protocol.

NO quantification

DAF-FM diacetate (4-amino-5-methylamino-2',7'-difluorofluorescein diacetate; Molecular Probes, Eugene, OR) was used to detect intracellular NO. DAF-FM diacetate is nonfluorescent until it crosses the cell membrane and becomes DAF-FM, and then interacts with NO to become a fluorescent benzotriazole (29,30). Cells were treated with 12 dyn/cm² of shear stress or static culture for 3 h prior to 10 μM of DAF-FM diacetate incubation. The dye was incubated for 30 min in 37°C and 5% CO₂, and then the samples were rinsed with PBS and incubated in M199 media for 15 min. Samples were imaged on a Zeiss LSM700 inverted laser scanning confocal microscope with a 10 \times objective (Carl Zeiss, Oberkochen, Germany). For all samples, a 488 nm laser was used to image 40.2 μm -deep sections for each sample. Twenty fields of view were taken per sample, and brightfield microscopy was used to ensure that the approximate cell count in each field of view was the same. Unstained cells were imaged to determine background fluorescence, which was subtracted from the fluorescent intensity values. Experiments were normalized over the range of fluorescent intensity values from the sheared glass sample in each experimental group, and data are presented where the control glass value was set to 0.5.

Statistical analysis

All analyses were performed using GraphPad Prism 5 (GraphPad Software, La Jolla, CA) or Excel 2010 (Microsoft, Redmond, WA). Student's *t*-tests or parametric one-way or two-way ANOVA with post hoc Tukey's honest significance test were performed where appropriate, and *p*-values < 0.05 were considered statistically significant.

RESULTS

Matrix compliance enhances EC alignment in response to fluid shear stress

To investigate the role of matrix stiffness in fluid shear stress-induced EC realignment, PA substrates mimicking young and aged arteries were seeded with ECs and placed in a cone-and-plate viscometer. After 24 h of shear at 12 dynes/cm², ECs align and elongate in the direction of fluid shear stress (Fig. 1, A and B), as expected based on pre-

vious work (1,31,32). Phase contrast images and fluorescent images of cells stained for actin and the nucleus indicate that cells align in the direction of fluid flow under all stiffness conditions after 24 h of shear. Interestingly, however, ECs on more compliant substrates under shear stress exhibit larger perimeters (Fig. 1 C) and greater elongation (Fig. 1 D) than cells on stiffer substrates. Other cell morphology parameters, such as total cell area and the extent of cell alignment relative to flow direction, are independent of substrate stiffness after 24 h of flow (Fig. S3).

Increased matrix stiffness inhibits fluid shear stress-induced barrier integrity

Fluid shear stress causes EC realignment, during which cell-cell junctions reform and barrier integrity is ultimately enhanced (33,34). Our previous data suggest that matrix

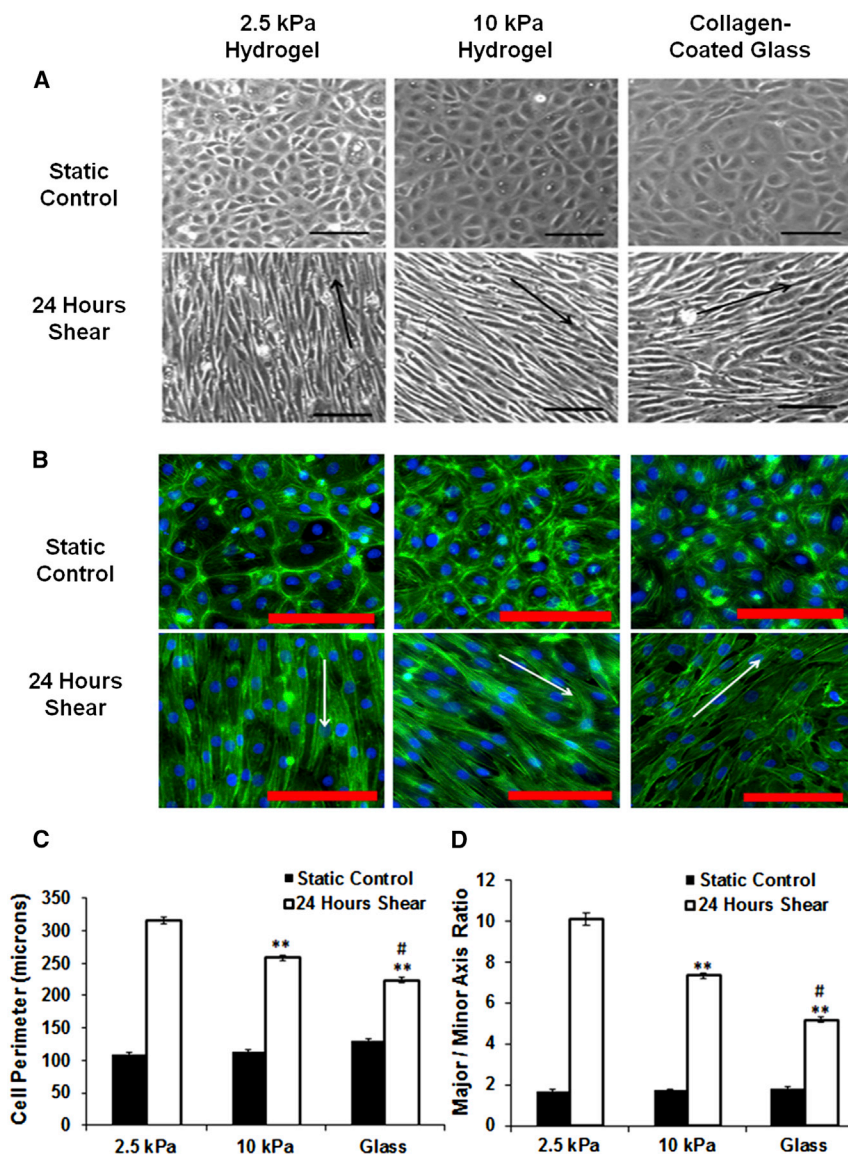


FIGURE 1 Matrix stiffness influences EC morphology under fluid shear stress. (A) Phase contrast images of ECs before and after shear stress exposure for 24 h at 12 dyn/cm². (B) Representative fluorescent images of actin fiber (green) and DAPI (blue) staining, showing reorganization of the actin network parallel to the flow direction. Arrows indicate approximate flow direction (see Supporting Material), and black/red scale bars are 100 μ m. (C and D) Quantification of EC perimeter and elongation. Data are mean \pm SE ($n = 180$ –350 cells for sheared cells, 30–40 cells for static controls, three independent experiments). ** $p < 0.01$ vs. 2.5 kPa sheared samples. # $p < 0.01$ vs. 10 kPa sheared samples, Tukey's test. To see this figure in color, go online.

stiffness disrupts barrier integrity by increasing traction stresses (6). Since fluid shear stress and matrix stiffness are both known to affect barrier integrity, we investigated their combined effects on EC-EC junctions. ECs were plated on hydrogels mimicking the stiffness of old and young arteries and subjected to 24 h of fluid shear stress. The samples were then immunostained for VE-cadherin, a cell-cell adhesion molecule responsible for maintaining EC junctions and mediating barrier function (35). ECs on the compliant 2.5 kPa substrate in static conditions display tighter cell-cell junctions compared with cells on 10 kPa substrates, similar to what we observed in our previous work (6). After 24 h of fluid shear stress, the junctions are tighter compared with static controls, and the tightest cell-cell junctions occur on compliant substrates (Fig. 2, A and B). This decrease in junctional gaps suggests that EC barrier function is enhanced by more compliant substrates under fluid shear stress. Interestingly, a comparison of EC morphology parameters, such as cell elongation (major/minor axis ratio) and cell perimeter, with junction width values indicates that EC elongation correlates with EC junction stabilization (Fig. 2 C). Also, on compliant substrates, junction integrity stabilizes after significant elongation has occurred, whereas this phenomenon is abrogated on stiffer substrates. As expected,

a relationship also exists between EC elongation and perimeter on both 2.5 kPa and 10 kPa substrates after fluid shear stress exposure (Fig. 2 C), although there are no notable correlations between EC junction width, area, perimeter, and elongation for static cultures (data not shown).

To further explore the mechanism by which EC-cell junctions are stabilized by compliant matrices and fluid shear stress, we focused on Rho-mediated signaling. The Rho/ROCK pathway has emerged as a mediator of EC barrier integrity and is strongly dependent on matrix stiffness (33,36). Activation of RhoA is required for actin reorganization and EC alignment under laminar fluid shear stress (37). Our data indicate that significant RhoA activation is present after 10 or 60 min of fluid shear stress for ECs cultured on stiff 10 kPa and glass substrates (Fig. 3), as previously shown for ECs cultured on glass (38). Notably, RhoA activation is significantly attenuated on the compliant 2.5 kPa hydrogels after 60 min of fluid shear stress.

Matrix stiffness mediates flow-induced ERK1/2 and eNOS activity

Fluid shear stress affects not only EC alignment and integrity but also a number of signaling pathways that regulate

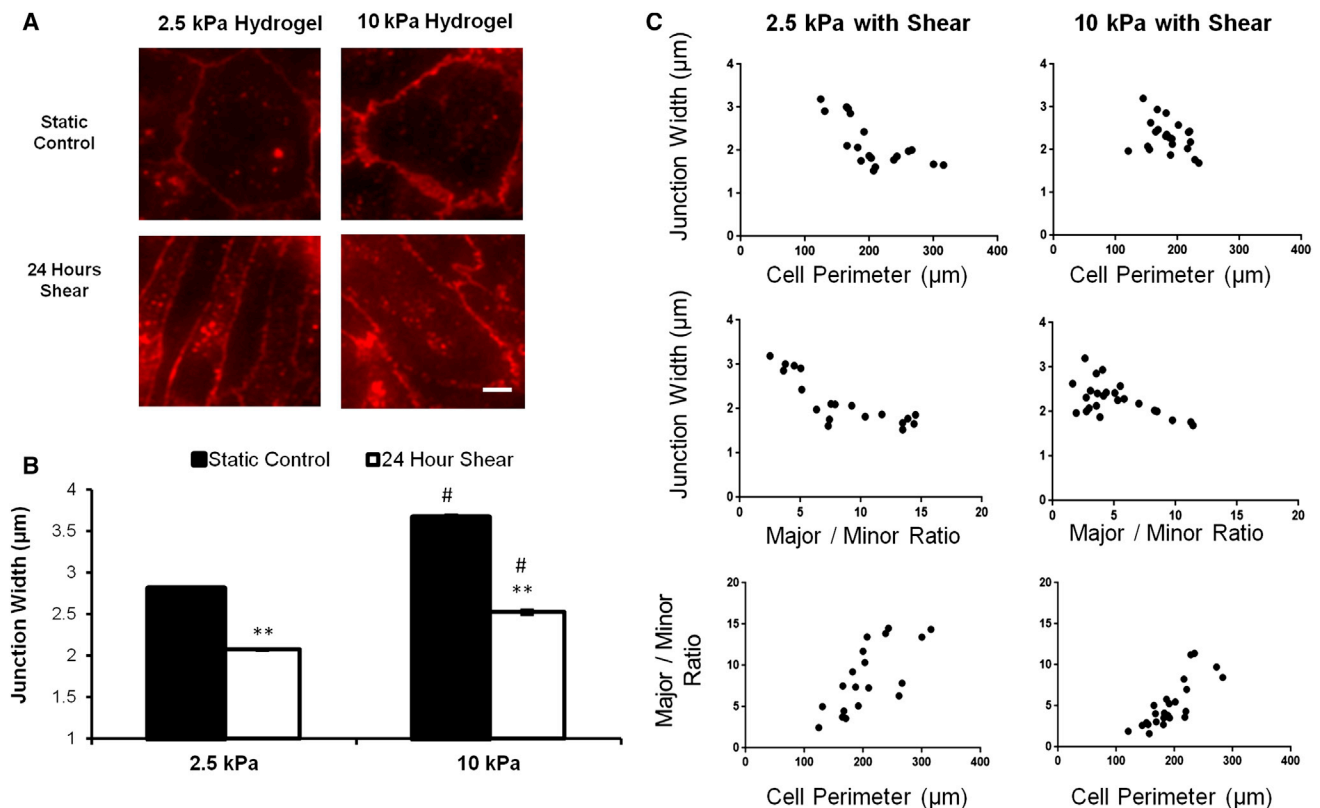


FIGURE 2 (A) Fluorescence images of VE-cadherin (red) of ECs on gels after shear stress exposure (12 dyn/cm^2 , 24 h) or static culture. Scale bar, $10 \mu\text{m}$. (B) VE-cadherin junction width measurements of BAECs on gels ($n > 150$ junction measurements, three independent experiments). Data are mean \pm SE. # $p < 0.01$, Tukey's test, compared with static condition; ** $p < 0.01$, Tukey's test, compared between stiffnesses. (C) Comparison of junction width, elongation (major/minor ratio), and cell perimeter. To see this figure in color, go online.

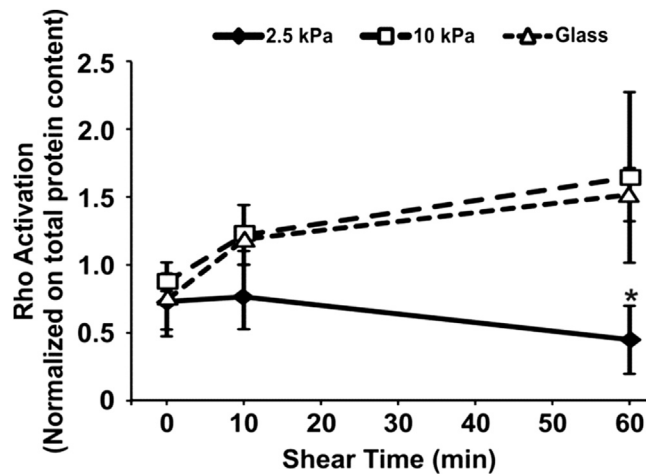


FIGURE 3 RhoA activation of ECs after 10 or 60 min of shear (12 dyn/cm²) or static culture. EC RhoA activation is greater on stiffer matrices at 60 min. Data are mean \pm SE, five replicates. * p < 0.05, Tukey's test, compared with 10 kPa and glass samples.

cell health. Several of these signaling molecules, including ERK1/2 and eNOS, are known to act through pathways that are also affected by matrix stiffness (21,22). We hypothesized that changes in matrix stiffness may alter signal transduction triggered by atheroprotective flow. Using glass substrates, others have shown that laminar flow in the physiological regime of 5–15 dyn/cm² increases both ERK1/2 and eNOS phosphorylation followed by a gradual decrease (3,4,39). Our data indicate that phosphorylation of both eNOS and Erk1/2 peaks within minutes of flow on all three stiffnesses (Fig. 4), as shown previously for ECs cultured on plastic or glass (3,4). The EC signaling response on 10 kPa gels closely mimics the response on glass (Fig. 4). Notably, however, ERK and eNOS phosphorylation peaks at 2 min on the 2.5 kPa hydrogels, whereas the phosphorylation peaks at 5 min on the 10 kPa hydrogels or glass (Fig. 4). These early ERK and eNOS phosphorylation peaks suggest that EC signaling is more sensitive to fluid shear stress on more compliant substrates.

To further explore whether these early signaling events result in physiological changes in the ECs, we measured NO production in response to shear stress as a function of matrix stiffness. Our data indicate that after 3 h of fluid shear stress, NO production is elevated in response to fluid shear and this response is enhanced on more compliant matrices (Fig. 5). These data suggest that compliant matrices augment the atheroprotective effects of fluid shear stress on ECs by increasing NO production.

DISCUSSION

Together, our results demonstrate a strong interplay between laminar fluid shear stress and matrix stiffness that affects EC health and function, and may contribute to atheroprone and atheroprotective EC phenotypes.

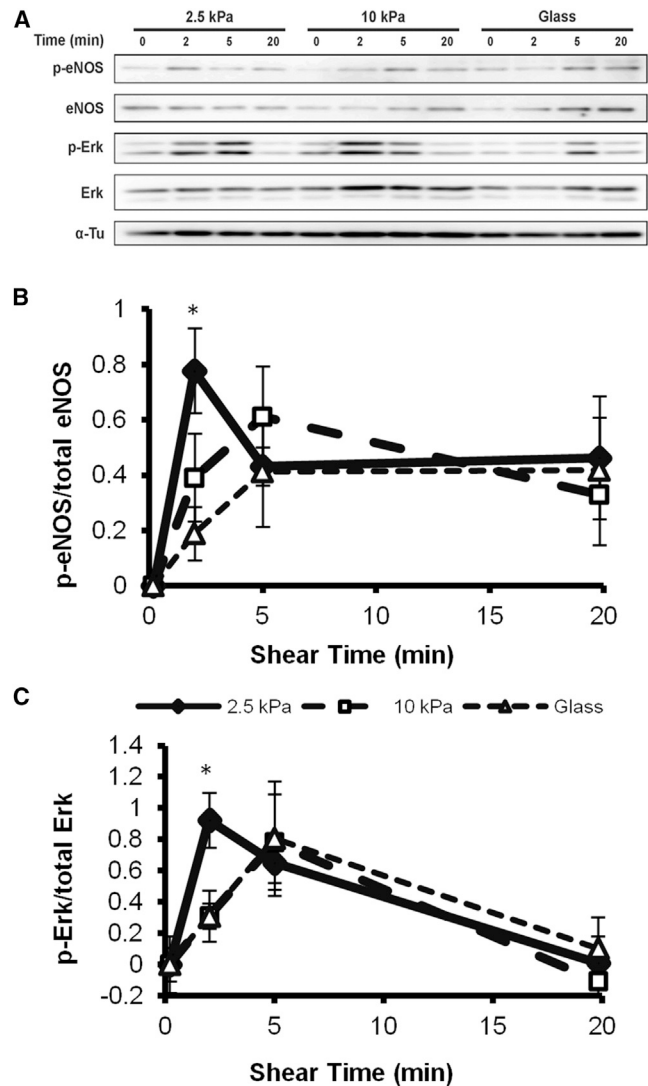


FIGURE 4 Matrix stiffness influences EC signaling induced by fluid shear stress. (A) Representative western blots for eNOS and ERK phosphorylation on matrices of varying stiffnesses after 12 dyn/cm² shear stress exposure for 0, 2, 5, and 20 min. α -Tubulin was used as the loading control. (B and C) Corresponding quantification of the phosphorylation level over time for both (B) eNOS Ser-1179 and (C) ERK Thr-202/Tyr-204 in response to fluid shear stress exposure (mean \pm SE, n = 4 for ERK, 5 for eNOS). * p < 0.05 vs. 10 kPa and glass (Tukey's test).

ECs become more elongated on compliant substrates after shear stress exposure. Although the process of EC elongation and alignment to fluid shear stress is not fully understood, Rho GTPase activity and cell traction stresses are known to modulate cell elongation and alignment (37). An initial increase in RhoA is needed for ECs under fluid shear to form stress fibers and for cells to orient in the flow direction. A decline in RhoA is then required for the cells to spread and elongate directionally (40). It was previously shown that decreased matrix stiffness results in decreased RhoA activity (6), and we demonstrate that this trend also occurs under fluid shear stress. Our

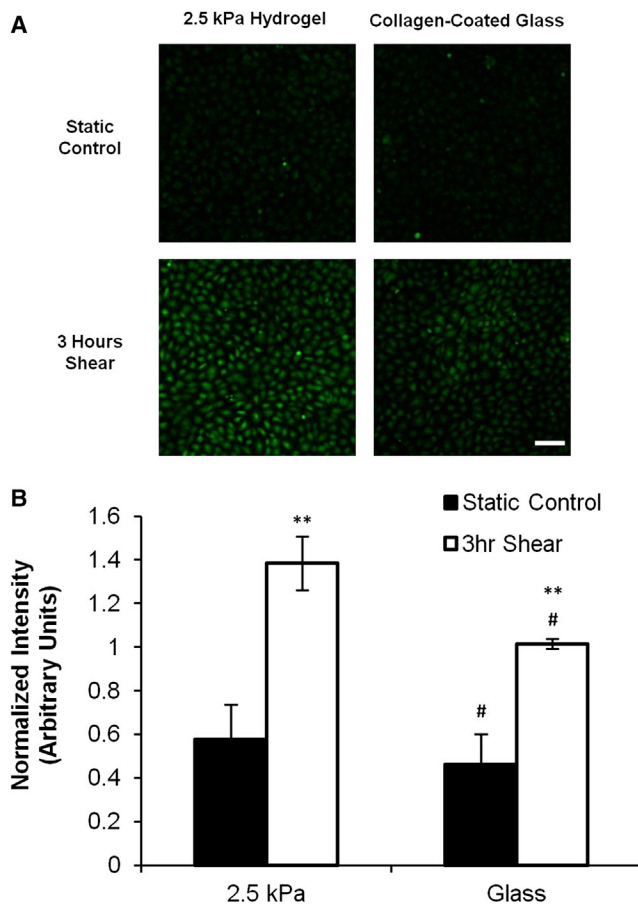


FIGURE 5 Matrix stiffness influences NO production induced by fluid shear stress. (A) Representative fluorescent images of ECs on 2.5 kPa gels or on collagen-coated glass stained with DAF-FM diacetate after 12 dyn/cm² shear stress exposure for 3 h or static conditions. Scale bar, 100 μ m. (B) Fluorescence quantification of samples normalized to glass shear from each experiment (mean \pm SE, $n = 3$ control samples and $n = 5$ sheared samples, 20 fields of view per sample). # $p < 0.005$ and ** $p < 0.02$ (Student's t -test). To see this figure in color, go online.

data support this model for the role of Rho in EC realignment to flow, where ECs elongate on compliant substrates and exhibit reduced RhoA activity. Since RhoA is known to mediate EC cell morphology (11,38,40), the lower RhoA values on the 2.5 kPa matrix may allow for increased EC elongation.

Our recent work indicates that ECs form tighter cell-cell junctions on more compliant matrices, strengthening the junctions and inducing an atheroprotective phenotype (6). The data presented here indicate that laminar shear stress exposure tightens EC junctions, and that this effect is augmented on more compliant substrates. Recent evidence suggests that cells tend to move in the direction of principal stresses (normal to the cell-cell junction) to avoid shearing along each other (41). We speculate that the compliant 2.5 kPa substrates used in our system may provide the optimal amount of Rho activation to allow cells to elongate without providing such strong cell-cell adhesion that the

cells are inhibited from moving adjacent to each other during the alignment process.

Previous studies have shown that ERK and eNOS phosphorylation is affected by fluid shear stress (3,16–18). Our ERK/eNOS data suggest that atheroprotective signaling events triggered by fluid shear stress occur earlier on more compliant matrices mimicking the mechanical properties of young and healthy blood vessels. Although the mechanism for this earlier activation remains unclear, we speculate that differences in EC cytoskeletal architecture between stiffnesses may be responsible. Shear-mediated ERK and eNOS activation has been shown to occur via cell-cell junction and focal adhesion signaling and remodeling (42,43). Since cells cultured on stiffer matrices typically exhibit more stabilized focal adhesions and cytoskeletal architectures (44) and wider gaps at cell-cell junctions (Fig. 2), ECs may require longer times to remodel these mechanosensory complexes to initiate signaling that leads to ERK and eNOS activation. This may account for the delayed ERK and eNOS activation that we observe on stiff matrices relative to compliant matrices, which exhibit more dynamic and diffuse focal adhesions and cytoskeletal architectures (44). It is important to note that we collected our data using steady flow. It is likely that physiological, pulsatile flow may augment this response even further.

CONCLUSIONS

Although the atheroprotective role of fluid shear stress is well documented, we demonstrate that matrix compliance also has an atheroprotective role that synergizes with fluid shear stress. When cultured on more compliant matrices under laminar fluid shear stress, ECs exhibit increased elongation, tighter cell-cell junctions, decreased Rho activation, and increased NO production. Our results reveal a critical role of matrix mechanics in mediating the EC response to fluid shear stress, and underscore the need to create more physiologically relevant models to study cell mechanotransduction.

SUPPORTING MATERIAL

Supporting Materials and Methods and three figures are available at [http://www.biophysj.org/biophysj/supplemental/S0006-3495\(14\)04770-5](http://www.biophysj.org/biophysj/supplemental/S0006-3495(14)04770-5).

AUTHOR CONTRIBUTIONS

J.C.K. and D.W.Z. designed and performed research, analyzed data, and wrote the article. F.B. performed research and analyzed data. A.L.Z. and B.N.M. performed research. M.J.M. and M.R.K. designed research and contributed analytic tools. C.A.R.-K. designed research, contributed analytic tools, and wrote the article.

ACKNOWLEDGMENTS

We gratefully acknowledge help and support from John Huynh, Shawn Carey, and Adeline Chen.

This work was supported by grants from the National Heart, Lung and Blood Institute (HL097296) and the National Science Foundation (1435755) to C.A.R.-K., and the National Science Foundation Graduate Research Fellowship Program to J.C.K. (2013165170).

SUPPORTING CITATIONS

Reference (45) appears in the [Supporting Material](#).

REFERENCES

- Malek, A. M., and S. Izumo. 1996. Mechanism of endothelial cell shape change and cytoskeletal remodeling in response to fluid shear stress. *J. Cell Sci.* 109:713–726.
- Zaragoza, C., S. Márquez, and M. Saura. 2012. Endothelial mechanosensors of shear stress as regulators of atherogenesis. *Curr. Opin. Lipidol.* 23:446–452.
- Boo, Y. C., G. Sorescu, ..., H. Jo. 2002. Shear stress stimulates phosphorylation of endothelial nitric-oxide synthase at Ser1179 by Akt-independent mechanisms: role of protein kinase A. *J. Biol. Chem.* 277:3388–3396.
- Jo, H., K. Sipos, ..., J. M. McDonald. 1997. Differential effect of shear stress on extracellular signal-regulated kinase and N-terminal Jun kinase in endothelial cells. $G\beta_2$ - and $G\beta/\gamma$ -dependent signaling pathways. *J. Biol. Chem.* 272:1395–1401.
- Chien, S. 2008. Effects of disturbed flow on endothelial cells. *Ann. Biomed. Eng.* 36:554–562.
- Huynh, J., N. Nishimura, ..., C. A. Reinhart-King. 2011. Age-related intimal stiffening enhances endothelial permeability and leukocyte transmigration. *Sci. Transl. Med.* 3:112–122.
- Isenberg, B. C., P. A. Dimilla, ..., J. Y. Wong. 2009. Vascular smooth muscle cell durotaxis depends on substrate stiffness gradient strength. *Biophys. J.* 97:1313–1322.
- Peyton, S. R., and A. J. Putnam. 2005. Extracellular matrix rigidity governs smooth muscle cell motility in a biphasic fashion. *J. Cell. Physiol.* 204:198–209.
- Huynh, J., F. Bordeleau, ..., C. A. Reinhart-King. 2013. Substrate stiffness regulates PDGF-induced circular dorsal ruffle formation through MLCK. *Cell Mol. Bioeng.* 6:138–147.
- Li, S., M. Kim, ..., J. Y. Shyy. 1997. Fluid shear stress activation of focal adhesion kinase. Linking to mitogen-activated protein kinases. *J. Biol. Chem.* 272:30455–30462.
- Tzima, E. 2006. Role of small GTPases in endothelial cytoskeletal dynamics and the shear stress response. *Circ. Res.* 98:176–185.
- Whited, B. M., and M. N. Rylander. 2014. The influence of electrospun scaffold topography on endothelial cell morphology, alignment, and adhesion in response to fluid flow. *Biotechnol. Bioeng.* 111:184–195.
- Paszek, M. J., N. Zahir, ..., V. M. Weaver. 2005. Tensional homeostasis and the malignant phenotype. *Cancer Cell.* 8:241–254.
- Koshida, R., P. Rocić, ..., W. M. Chilian. 2005. Role of focal adhesion kinase in flow-induced dilation of coronary arterioles. *Arterioscler. Thromb. Vasc. Biol.* 25:2548–2553.
- Li, H., S. Horke, and U. Förstermann. 2014. Vascular oxidative stress, nitric oxide and atherosclerosis. *Atherosclerosis.* 237:208–219.
- Kimura, H., N. Okubo, ..., A. Ishisaki. 2013. EGF positively regulates the proliferation and migration, and negatively regulates the myofibroblast differentiation of periodontal ligament-derived endothelial progenitor cells through MEK/ERK- and JNK-dependent signals. *Cell. Physiol. Biochem.* 32:899–914.
- Sumpio, B. E., S. Yun, ..., J. A. Madri. 2005. MAPKs (ERK1/2, p38) and AKT can be phosphorylated by shear stress independently of platelet endothelial cell adhesion molecule-1 (CD31) in vascular endothelial cells. *J. Biol. Chem.* 280:11185–11191.
- Bretón-Romero, R., C. González de Orduña, ..., S. Lamas. 2012. Critical role of hydrogen peroxide signaling in the sequential activation of p38 MAPK and eNOS in laminar shear stress. *Free Radic. Biol. Med.* 52:1093–1100.
- Laboureau, J., L. Dubertret, ..., B. Coulomb. 2004. ERK activation by mechanical strain is regulated by the small G proteins rac-1 and rhoA. *Exp. Dermatol.* 13:70–77.
- Takeda, H., K. Komori, ..., K. Naruse. 2006. Bi-phasic activation of eNOS in response to uni-axial cyclic stretch is mediated by differential mechanisms in BAECs. *Life Sci.* 79:233–239.
- Mavria, G., Y. Vercoulen, ..., C. J. Marshall. 2006. ERK-MAPK signaling opposes Rho-kinase to promote endothelial cell survival and sprouting during angiogenesis. *Cancer Cell.* 9:33–44.
- Ming, X. F., H. Viswambharan, ..., Z. Yang. 2002. Rho GTPase/Rho kinase negatively regulates endothelial nitric oxide synthase phosphorylation through the inhibition of protein kinase B/Akt in human endothelial cells. *Mol. Cell. Biol.* 22:8467–8477.
- Califano, J. P., and C. A. Reinhart-King. 2008. A balance of substrate mechanics and matrix chemistry regulates endothelial cell network assembly. *Cell. Mol. Bioeng.* 1:122–132.
- Peloquin, J., J. Huynh, ..., C. A. Reinhart-King. 2011. Indentation measurements of the subendothelial matrix in bovine carotid arteries. *J. Biomech.* 44:815–821.
- Sdougos, H. P., S. R. Bussolari, and C. F. Dewey. 1984. Secondary flow and turbulence in a cone-and-plate device. *J. Fluid Mech.* 138:379–404.
- Fewell, M. E. 1977. The secondary flow of Newtonian fluids in cone-and-plate viscometers. *J. Rheol.* 21:535.
- Rezakhaniha, R., A. Agianniotis, ..., N. Stergiopoulos. 2012. Experimental investigation of collagen waviness and orientation in the arterial adventitia using confocal laser scanning microscopy. *Biomech. Model. Mechanobiol.* 11:461–473.
- van Nieuw Amerongen, G. P., C. M. L. Beckers, ..., V. W. M. van Hinsbergh. 2007. Involvement of Rho kinase in endothelial barrier maintenance. *Arterioscler. Thromb. Vasc. Biol.* 27:2332–2339.
- Kojima, H., N. Nakatsubo, ..., T. Nagano. 1998. Detection and imaging of nitric oxide with novel fluorescent indicators: diaminofluoresceins. *Anal. Chem.* 70:2446–2453.
- Kojima, H., K. Sakurai, ..., T. Nagano. 1998. Development of a fluorescent indicator for nitric oxide based on the fluorescein chromophore. *Chem. Pharm. Bull. (Tokyo).* 46:373–375.
- Nerem, R. M., M. J. Levesque, and J. F. Cornhill. 1981. Vascular endothelial morphology as an indicator of the pattern of blood flow. *J. Biomech. Eng.* 103:172–176.
- Levesque, M. J., and R. M. Nerem. 1985. The elongation and orientation of cultured endothelial cells in response to shear stress. *J. Biomech. Eng.* 107:341–347.
- Wojciak-Stothard, B., and A. J. Ridley. 2003. Shear stress-induced endothelial cell polarization is mediated by Rho and Rac but not Cdc42 or PI 3-kinases. *J. Cell Biol.* 161:429–439.
- Melchior, B., and J. A. Frangos. 2010. Shear-induced endothelial cell-cell junction inclination. *Am. J. Physiol. Cell Physiol.* 299:C621–C629.
- Dejana, E., E. Tournier-Lasserre, and B. M. Weinstein. 2009. The control of vascular integrity by endothelial cell junctions: molecular basis and pathological implications. *Dev. Cell.* 16:209–221.
- Birukova, A. A., X. Tian, ..., K. G. Birukov. 2013. Endothelial barrier disruption and recovery is controlled by substrate stiffness. *Microvasc. Res.* 87:50–57.
- Shiu, Y. T., S. Li, ..., S. Chien. 2004. Rho mediates the shear-enhancement of endothelial cell migration and traction force generation. *Biophys. J.* 86:2558–2565.
- Tzima, E., M. A. del Pozo, ..., M. A. Schwartz. 2001. Activation of integrins in endothelial cells by fluid shear stress mediates Rho-dependent cytoskeletal alignment. *EMBO J.* 20:4639–4647.
- Barauna, V. G., P. R. Mantuan, ..., J. E. Krieger. 2013. AT1 receptor blocker potentiates shear-stress induced nitric oxide production

- via modulation of eNOS phosphorylation of residues Thr(495) and Ser(1177). *Biochem. Biophys. Res. Commun.* 441:713–719.
40. Wójciak-Stothard, B., and A. J. Ridley. 2002. Rho GTPases and the regulation of endothelial permeability. *Vascul. Pharmacol.* 39:187–199.
 41. Treppe, X., and J. J. Fredberg. 2011. Plithotaxis and emergent dynamics in collective cellular migration. *Trends Cell Biol.* 21:638–646.
 42. Fleming, I., B. Fisslthaler, ..., R. Busse. 2005. Role of PECAM-1 in the shear-stress-induced activation of Akt and the endothelial nitric oxide synthase (eNOS) in endothelial cells. *J. Cell Sci.* 118:4103–4111.
 43. Tzima, E., M. Irani-Tehrani, ..., M. A. Schwartz. 2005. A mechanosensory complex that mediates the endothelial cell response to fluid shear stress. *Nature.* 437:426–431.
 44. Pelham, Jr., R. J., and Yl. Wang. 1997. Cell locomotion and focal adhesions are regulated by substrate flexibility. *Proc. Natl. Acad. Sci. USA.* 94:13661–13665.
 45. Traub, O., and B. C. Berk. 1998. Laminar shear stress: mechanisms by which endothelial cells transduce an atheroprotective force. *Arterioscler. Thromb. Vasc. Biol.* 18:677–685.